Theor Chem Acc (2009) 123:337–346
DOI 10.1007/s00214-009-0521-4

REGULAR ARTICLE

Stepwise versus concerted mechanisms in the Wittig reaction in vacuo and in THF: the case of 2,4-dimethyl-3-pyrrol-1-yl-pentanal and triphenylphosphonium ylide

Giuliano Alagona · Caterina Ghio

Received: 17 November 2008 / Accepted: 24 January 2009 / Published online: 22 February 2009

Abstract The Wittig reaction of the unsubstituted triphenylphosphonium ylide (Ph_3PCH_2) on an aldehyde with two stereogenic centers ((2*S*,3*R*)-2,4-dimethyl-3-pyrrol-1-yl-pentanal) has been investigated with a density functional approach at the B3P86/6-31G* level in vacuo and in tetrahydrofuran (THF) to shed some light on the mechanistic details when bulky chiral substrates are employed in the absence of E/Z selectivity issues. The interest is focused on the reaction intermediates, primarily on those that cannot be observed spectroscopically. Both the concerted mechanism (with a four-center transition state (TS)) and the stepwise one (occurring via a betaine-type zwitterionic intermediate) have been explored, examining the potential energy profiles as well as the free energy ones. The solvent effect in the integral equation formalism-polarizable continuum model (IEF-PCM) framework has also been considered for THF. Interestingly, the early TS found in vacuo for both mechanisms becomes vanishingly small in THF, while the reactant adducts turn out to be somewhat destabilized, with an overall similarity in the relevant profiles.

Keywords Density functional calculations · B3P86/6-31G* · IEF-PCM · Reaction mechanisms · Wittig reaction · Oxaphosphetane · Betaine

Dedicated to the memory of Professor Oriano Salvetti and published as part of the Salvetti Memorial Issue.

Electronic supplementary material The online version of this article (doi:10.1007/s00214-009-0521-4) contains supplementary material, which is available to authorized users.

G. Alagona (✉) · C. Ghio
IPCF, CNR, Molecular Modelling Lab.,
Via Moruzzi 1, 56124 Pisa, Italy
e-mail: G.Alagona@ipcf.cnr.it

C. Ghio
e-mail: C.Ghio@ipcf.cnr.it

1 Introduction

The Wittig reaction [1–3] is an important organic transformation that has received and continues receiving wide attention, especially concerning its E/Z selectivity (see Fig. 1), from both experimental [4–12] and theoretical [13–21] viewpoints. This reaction converts a C=O double bond to a C=C double bond using a phosphorus ylide (or a phosphorane) with good selectivity when non-methylenic ylides (i.e. with $R_1 \neq H$) are used, depending on the nature of R_1 [10, 11, 15–18]. Therefore, in those investigations, emphasis was put on the ylide rather than on the aldehyde.[1]

Despite the importance of this reaction in organic synthesis, testified by the Nobel Prize for Chemistry awarded to Georg Wittig in 1979, its mechanism is still under debate. The question of formation of oxaphosphetane (OP) or betaine-type intermediates (displayed in Fig. 2) has been addressed by means of experimental and computational methods without a clear answer. The betaine intermediate has been isolated as a lithium salt, but not as a true betaine [4].

Some of the aforementioned studies support the formation of OP either directly [5–8, 17, 18, 22] or via a betaine-type intermediate [4], others claim that betaine is the only intermediate [23]. Furthermore Vedejs has argued [7] and eventually offered evidence [8] that the reaction passes through a four-centered transition state (TS) leading

[1] The reaction occurs with ketones or epoxide rings [4, 22] as well, although it is less facile because of steric hindrance.

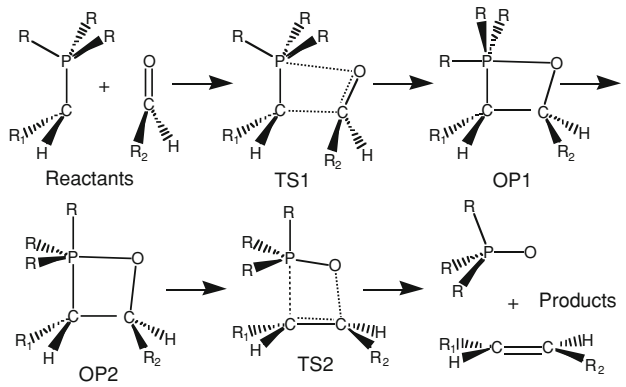

Fig. 1 Schematic representation of the Wittig reaction through oxaphosphetanes (OP)

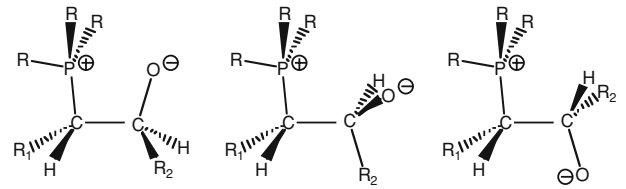

Fig. 2 Schematic representation of syn (*left*), gauche (*middle*) and anti (*right*) betaine-type structures

directly to an OP and not through a betaine, at least for the considered systems and conditions. However, since the purpose of this paper is not to review the literature, we refer the readers to a number of review articles [24–27] and limit ourselves to mention specific mechanistic studies.

Here, attention is focused on reaction steps and intermediates when the reaction involves the triphenylphosphonium ylide (Ph_3PCH_2) and a peculiar bulky compound, such as a chiral aldehyde (2,4-dimethyl-3-pyrrol-1-yl-pentanal; Fig. 3), because the only fact clearly emerging from the literature on the Wittig reaction is the difficulty to infer adequate and reliable mechanistic details from model systems, despite it was claimed that they should provide results applicable to Ph_3PCH_2 at least [21]. Preliminary calculations on $(CH_3)_3PCH_2$–CH_3CHO and Ph_3PCH_2–CH_3CHO, as model systems, produced different and sometimes conflicting results without a conclusive answer [28]. Therefore, we decided to study the mechanism on a realistic system with two chiral centers. Obviously, there is an ample choice of such compounds. This particular diastereomeric aldehyde was brought to our attention by organic colleagues who synthesized it via a hydroformylation reaction while seeking for a particular regio- and diastereoselectivity. Like all the aldehydes with a chiral group in α position, this compound is however configurationally unstable because of the keto–enol equilibrium. To prevent racemization of the chiral group before its

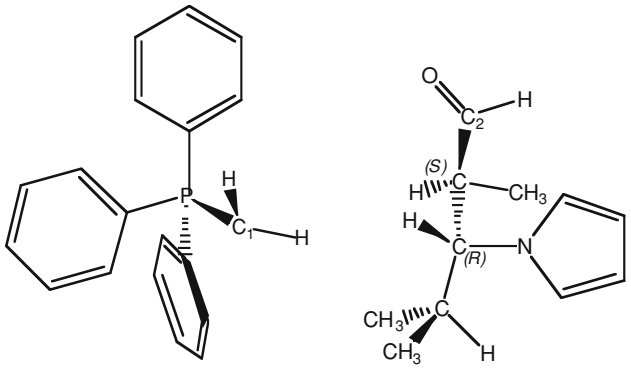

Fig. 3 Schematic representations of Ph_3PCH_2 (*left*) and (2*S*,3*R*)-2,4-dimethyl-3-pyrrol-1-yl-pentanal (*right*), both sketched without aromatic ring hydrogens

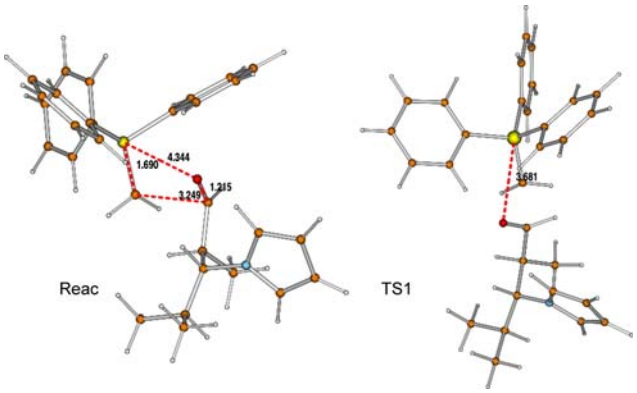

Fig. 4 B3P86/6-31G* structures along the reaction pathway: reactant adduct (Reac) between Ph_3PCH_2 and (2*S*,3*R*)-2,4-dimethyl-3-pyrrol-1-yl-pentanal (AldSR) and TS1

characterization, a common strategy consists in transforming the crude hydroformylation mixture into the corresponding olefins with an additional C atom exploiting the Wittig methylenation carried out at 25 °C [29]. This mechanistic investigation has been carried out in vacuo and in tetrahydrofuran (THF) solution in the framework of the integral equation formalism-polarizable continuum model (IEF-PCM), including thermal corrections both in the gas phase and in solution.

2 Computational details

All the calculations have been carried out with the Gaussian 03 system of programs [30] in the density functional theory (DFT) framework, making use of a hybrid method, B3P86 [31, 32], and of the 6-31G* basis set [33] (6d description). We resorted to the B3P86 functionals because they were successfully used in our previous studies on the regio- and diastereoselectivity of the Rh-catalyzed hydroformylation of the several olefins [34–38], including

Table 1 B3P86/6-31G* relative energies (kcal/mol) in vacuo and some geometrical parameters (Å and deg)

System	ΔE[a]	PC_1	PO	C_1C_2	C_2O	PC_1C_2O	POC_2C_1	$\Delta G(298)$[b]
Ph_3PCH_2[c]		1.682	–	–	–	–	–	–
AldSR[d]		–	–	–	1.209	–	–	–
Reac	−4.756	1.690	4.344	3.249	1.215	45.61	−16.00	6.682
TS1	−2.297	1.730	3.681	2.276	1.245	40.06	−16.62	14.067
OP1	−29.973	1.872	1.826	1.522	1.419	15.31	−15.54	−10.673
OP2	−24.729	1.962	1.705	1.511	1.452	6.76	−7.89	−4.324
TS2	−5.515	2.439	1.573	1.408	1.851	3.54	−5.53	11.508
Prod[e]	−47.338	–	1.501	1.332	–	–	–	−45.247

[a] Ref. energy = $-1{,}639.337848E_h$

[b] Ref. free energy at 298 K and 1 atm = $-1{,}638.861011E_h$

[c] Energy = $-1{,}078.199295E_h$

[d] Energy = $-561.138553E_h$

[e] Prod stands for the isolated products: Ph_3PO and (3*R*,4*R*)-3,5-dimethyl-4-pyrrol-1-yl-hex-1-ene

Table 2 B3P86/6-31G* relative energies (kcal/mol) in vacuo and some geometrical parameters (Å) of higher minima and TS

System	ΔE	PC_1	PO	C_1C_2	C_2O	PC_1C_2O	POC_2C_1
Reac(p−)	−3.937	1.698	4.866	3.243	1.213	−66.24	14.46
TS1(p−)	1.911	1.751	3.877	2.081	1.253	−73.08	22.38
Reac(p+)	−1.301	1.687	4.091	3.758	1.212	60.36	−20.73
TS1(p+)	−1.084	1.727	3.359	2.264	1.243	25.43	−12.47

the substrate that yielded 2,4-dimethyl-3-pyrrol-1-yl-pentanal [38]. Thermal corrections for obtaining standard free energies at T = 298 K and 1 atm for the various stationary points located on the potential energy surface (PES) were calculated using the rigid rotator-harmonic oscillator approximation [39]:

$$G(T) = E(0) + \mathrm{ZPE} + \Delta H(0-T) - T\Delta S(0-T).$$

The solvent has been considered in the integral equation formalism of the polarizable continuum model (IEF-PCM) framework [40–46]. The cavity surrounding the solute, used to formulate the basic electrostatic equations characterizing the solute–solvent interactions, is the result of the superimposition of interlocking spheres centered on atomic sites with scaled[2] Bondi radii [47], apart from the CH_n groups, modeled with scaled (see footnote 2) united-atom radii ($R(CH_3) = R(CH_2) = 2.0$ Å, $R(CH) = 1.9$ Å). The total free energy in solution is computed as

$$G_{\mathrm{tot}}(0) = G_{\mathrm{elst}} + G_{\mathrm{dis}} + G_{\mathrm{rep}} + G_{\mathrm{cav}} = G_{\mathrm{elst}} + G_{\mathrm{drc}}$$

where the subscripts elst, dis, rep, cav, and drc stand for electrostatic, dispersion, repulsion, cavitation, and dispersion–repulsion–cavitation, respectively.

[2] A scaling factor of 1.2 was applied. For the sake of clarity, the original unscaled Bondi values are as follows: $R(C) = 1.7$ Å, $R(N) = 1.55$ Å, $R(O) = 1.52$ Å, and $R(P) = 1.8$ Å.

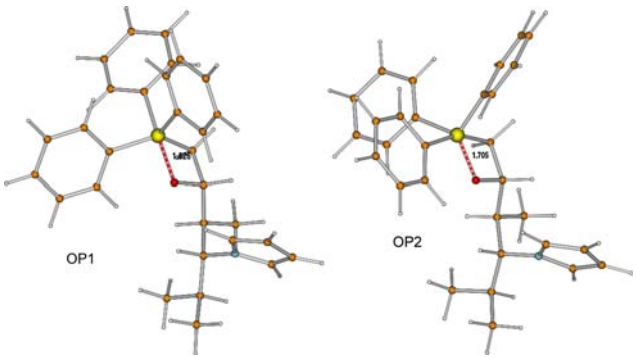

Fig. 5 B3P86/6-31G* structures of the oxaphosphetanes: OP1 and OP2

All stationary points have been characterized by computing vibrational frequencies in vacuo and in THF solution. In the latter case, $G_{\mathrm{tot}}(T)$ is calculated, in analogy to the in vacuo procedure, by adding the thermal corrections in solution on the solute geometry optimized in THF solution to the total free energy:

$$G_{\mathrm{tot}}(T) = G_{\mathrm{tot}}(0) + [\mathrm{ZPE} + \Delta H(0-T) - T\Delta S(0-T)]_{\mathrm{THF}}.$$

3 Results and discussion

3.1 Concerted reaction mechanism in vacuo

The approaching path of Ph_3PCH_2 to (2*S*,3*R*)-2,4-dimethyl-3-pyrrol-1-yl-pentanal (AldSR) has been thoroughly investigated in order to find the reactant lowest energy adduct (Reac), displayed in Fig. 4. Reac is more stable by 4.76 kcal/mol than the partners at infinite separation and is characterized by a PC_1C_2O dihedral angle of 45.6°. This

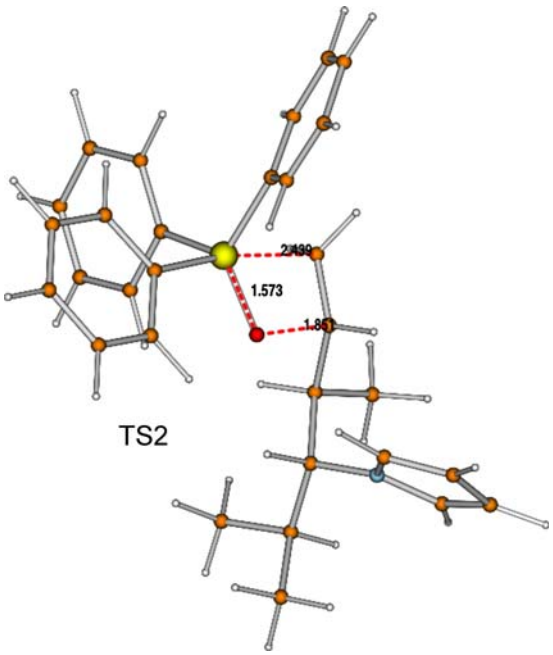

Fig. 6 B3P86/6-31G* structure of TS2

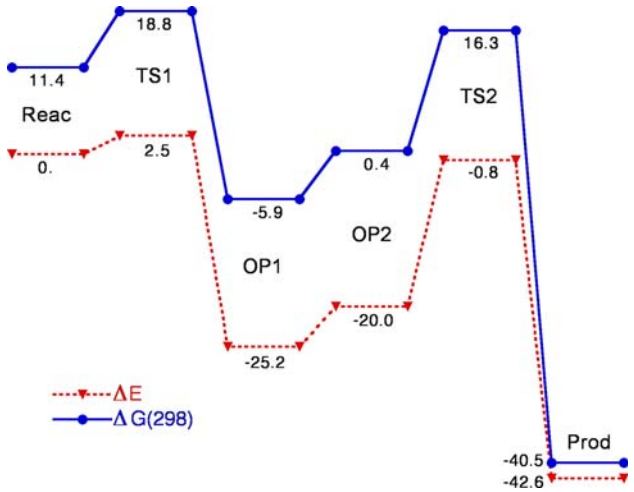

Fig. 7 B3P86/6-31G* profiles (kcal/mol) along the concerted pathway in vacuo: potential energy, *E* (*dotted line*, *down triangles*) and free energy at 298 K, *G* (*solid line*, *circles*) with respect to the potential energy of Reac taken as zero

puckering is likely due to the steric hindrance of the substituents at P and at the carbonyl C. The corresponding transition state (TS1), also displayed in Fig. 4, is still more stable than the isolated partners by 2.30 kcal/mol and the puckering is maintained. Some geometrical parameters are reported in Table 1 for all the selected stationary points.

In our search, other minimum energy structures have been located, especially for reactant adducts and the first TS because of the large intermolecular distance and the compound flexibility, although somewhat higher in energy.

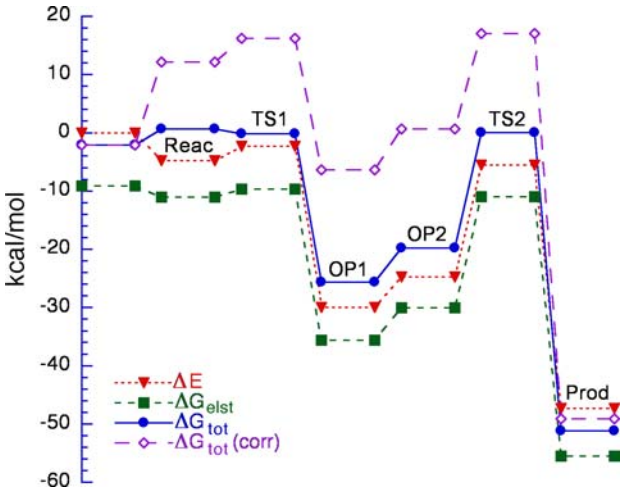

Fig. 8 IEF-PCM/B3P86/6-31G*//B3P86/6-31G* free energy profiles in THF along the concerted pathway: ΔG_{elst} (*short dashes*, *squares*), ΔG_{tot} (*solid line*, *circles*) and ΔG_{tot}(corr) (see text, *long dashes*, *diamonds*). The potential energy in vacuo ΔE (*dotted line*, *down triangles*) is also displayed for comparison

Two couples of those stationary points (named p− and p+ depending on their PCCO values) are reported in Table 2.

Once TS1 has been reached, geometry optimization to a minimum leads to OP1, displayed in Fig. 5, a trigonal–bipyramidal (TBP) structure at P, with O and one of the phenyl rings in apical position. The pseudorotation of the groups at P produces OP2, a TBP structure as well with CH_2 and another phenyl ring in apical position. The TS between OP1 and OP2 is very late and practically coincides with OP2.

The final transition state, TS2, displayed in Fig. 6, is lower in energy than the reactant adduct, and features a quasi-planar arrangement for the PO and CC four centers. The energy profile along the whole reaction pathway is displayed in Fig. 7 (dotted line).

The final step yields the products (remarkably more stable than the initial adduct) which consist of triphenylphosphoxide and the olefin corresponding to the aldehyde, with an additional carbon atom on the main chain, i.e. (3*R*,4*R*)-3,5-dimethyl-4-pyrrol-1-yl-hex-1-ene,[3] in this case.

Before discussing the solvent effect on the reaction profile, it is advisable to take into account the free energy along the pathway in vacuo. All the frequencies are real for the minima, whereas one imaginary frequency (iF) is obtained for TS1 and TS2 (-82.31 and -486.61 cm^{-1}, respectively). The TS very close to OP2 conversely has a small imaginary frequency (iF $= -11.46$ cm^{-1}), testifying its ambiguous nature. By comparing the free energy profile

[3] The change in the chirality is due to the Cahn–Ingold–Prelog priority rules.

Table 3 IEF-PCM/B3P86/6-31G* relative total free energies (kcal/mol) in THF and some geometrical parameters (Å and deg)

System	ΔG^{a}_{tot}	PC_1	PO	C_1C_2	C_2O	PC_1C_2O	POC_2C_1	$\Delta G_{tot}(298)^{b}$
$Ph_3PCH_2^{c}$		1.683	–	–	–	–	–	–
AldSR[d]		–	–	–	1.213	–	–	–
Reac	2.799	1.692	4.526	3.283	1.216	50.91	−17.16	14.116
Reac(T)	2.929	1.693	4.553	3.223	1.217	36.54	−12.11	13.625
OP1	−23.547	1.869	1.836	1.522	1.420	12.16	−12.45	−4.165
TS2	2.179	2.440	1.575	1.409	1.841	3.59	−5.59	19.533
Prod[e]	−48.990	–	1.508	1.333	–	–	–	−46.785

[a] Ref. total free energy = $-1{,}639.341304E_h$

[b] Ref. $G_{tot}(298) = -1{,}638.865948E_h$

[c] Energy = $-1{,}078.199286E_h$

[d] Energy = $-561.142018E_h$

[e] Prod stands for the isolated products

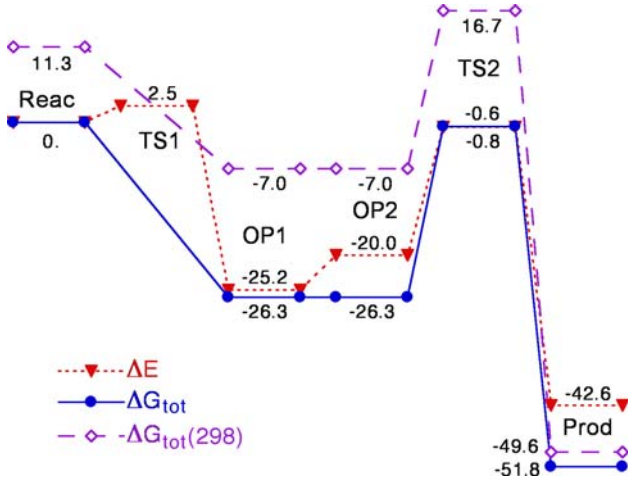

Fig. 9 IEF-PCM/B3P86/6-31G* free energy profiles (kcal/mol) in THF along the concerted pathway: ΔG_{tot} (*solid line*, *circles*) and $\Delta G_{tot}(298)$ (*dashed line*, *diamonds*). The potential energy in vacuo, ΔE (*dotted line*, *down triangles*), is also displayed for comparison

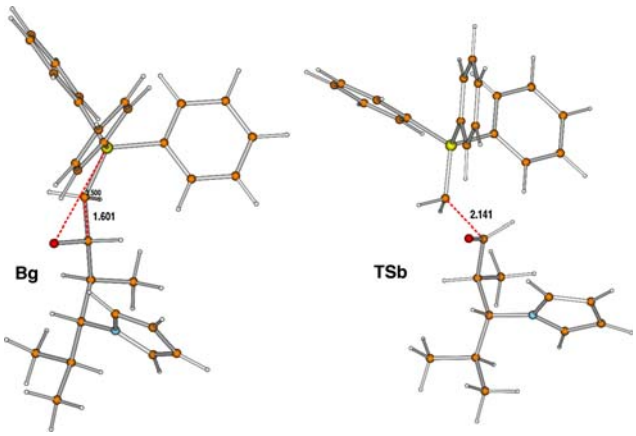

Fig. 10 B3P86/6-31G* structure of the gauche betaine-type intermediate (Bg) between Ph_3PCH_2 and (2*S*,3*R*)-2,4-dimethyl-3-pyrrol-1-yl-pentanal and the transition state (TSb) to reach it from Reac(B)

(also displayed in Fig. 7, solid line) to the potential energy one, it is evident that the primary differences between them depend on the system molecularity and on the fact that Reac on the free energy surface[4] is along the uphill pathway leading to TS1. Concerning the molecularity, when the number of molecules decreases, there is a significant increment (ranging from 11.5 to 20.5 kcal/mol) in the free energy that is roughly maintained till the final TS. When the products are released returning to two separate molecules, there is a remarkable gain in free energy [the relative free energy[5] of the products with respect to the isolated reactants is −45.3 kcal/mol in vacuo, just 2.1 kcal/mol less favorable than their potential energy (−47.4 kcal/mol)]. Therefore, the free energy profile for all the intermediate steps corresponding to stable complexes and connecting TS is much higher than the potential energy profile.

3.2 Concerted reaction mechanism in THF

Two different approaches have been used to consider solvent effects in the IEF-PCM framework. The first one consists in embedding the rigid partners in solution, while in the second approach the solute structures have been allowed to relax. The solvent used is THF ($\varepsilon = 7.58$).

3.2.1 In vacuo rigid geometries

This is the most commonly used procedure for studying solvent effects, employed also in [18]. Embedding the

[4] Probably there is a TS between isolated partners and the Reac adduct (the Reac adduct can be just a shallow minimum on the free energy surface).

[5] Named $\Delta G(298)$ whereas $\Delta G_{tot}(298)$ stands for the free energy in THF solution.

Table 4 B3P86/6-31G* relative energies in vacuo and geometrical parameters of betaine-type structures

System	ΔE	PC_1	PO	C_1C_2	C_2O	PC_1C_2O	POC_2C_1	$\Delta G(298)$
Reac(B)	−4.103	1.699	4.783	3.210	1.213	80.41	−17.53	5.474
TSb	−0.761	1.745	3.939	2.141	1.248	86.33	−24.43	15.230
Bg	−6.594	1.812	3.500	1.601	1.325	86.98	−34.41	10.084
TS(Bg–OP1)	−6.480	1.817	3.394	1.591	1.327	80.34	−34.40	21.690
OP1	−29.206	1.872	1.834	1.527	1.415	11.57	−11.87	−10.464
TS(Ba–Bg)	6.285	1.815	4.020	1.659	1.303	141.86	−20.94	23.545
Ba	5.581	1.822	4.093	1.660	1.301	168.97	−6.18	22.252

Relative energies (kcal/mol), distances (Å), angles (deg); reference values in Table 1

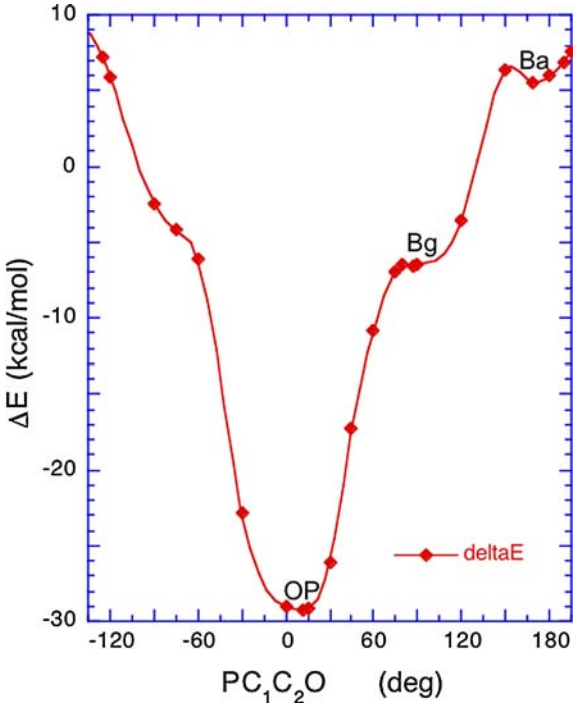

Fig. 11 B3P86/6-31G* flexible scan about PC_1C_2O in vacuo starting from the gauche betaine-type intermediate (Bg) between Ph_3PCH_2 and (2*S*,3*R*)-2,4-dimethyl-3-pyrrol-1-yl-pentanal

various arrangements of the rigid partners in THF solution, a similar electrostatic solvent effect (G_{elst}) is obtained for each species, whereas the inclusion of cavitation–dispersion–repulsion terms, leading to G_{tot}, remarkably destabilizes the reactant adduct, as can be derived from the profiles plotted in Fig. 8. This destabilizing effect[6] causes the reactant adduct to become less stable than TS1, while the general trend of the profiles is conserved. The magnitude of total and electrostatic solvent effects can be inferred from their separation from the in vacuo values.

Interestingly, with rigid geometries in solution, despite a bulky substrate has been used, the results are consistent with those obtained for HCHO and CH_3CHO [18]. Including zero point and thermal corrections in vacuo, i.e. $\Delta G(298)$, the corrected free energy profile in THF ($\Delta G_{tot}(corr)$) is obtained. However, to better elucidate the solvent effects, the solute structures have been optimized in solution.

3.2.2 *Geometries optimized in THF*

The geometries have been allowed to relax in solution starting from the structures optimized in vacuo as a standard procedure. Nevertheless this was not the only methodological approach followed, because the optimizations in solution presented several problems due to the system dimensions, the number of degrees of freedom and the cavity shape. It was indeed a difficult task to reach convergence. In particular, a lot of efforts were undertaken to optimize TS1 and the reactant adduct. Despite a huge number of attempts, even considering the alternative geometries found for TS1 (see Table 2), all runs eventually ended producing structures similar either to OP1 or Reac, that however were definitely useless because the optimizations had been carried out looking for TS. OP2 as well returned invariably to a solvated OP1-type structure. This kind of behavior clearly indicates that in THF solution the barrier between OP2 and OP1 as well as that related to TS1 is too low to be located, because it is easily surmounted by optimization algorithms. Therefore, the stationary points located in THF for the concerted mechanism are reported in Table 3, while in Fig. 9 the profile in THF solution is compared to the in vacuo one (with respect to Reac taken as zero).

Of course the steps have been plotted equally spaced as in vacuo: this, however, does not imply at all an analogous shape in the PES, where the minimum energy path can be smoother or steeper depending on the separation between the stationary points. It appears anyway evident that the concerted profile in solution presents a minimum basin

[6] Responsible for this effect is the cavitation term, because to this end the cavity is built using bare vdW radii without additional spheres; thus, due to the significant intermolecular separation between the partners, a large cavity surface is produced.

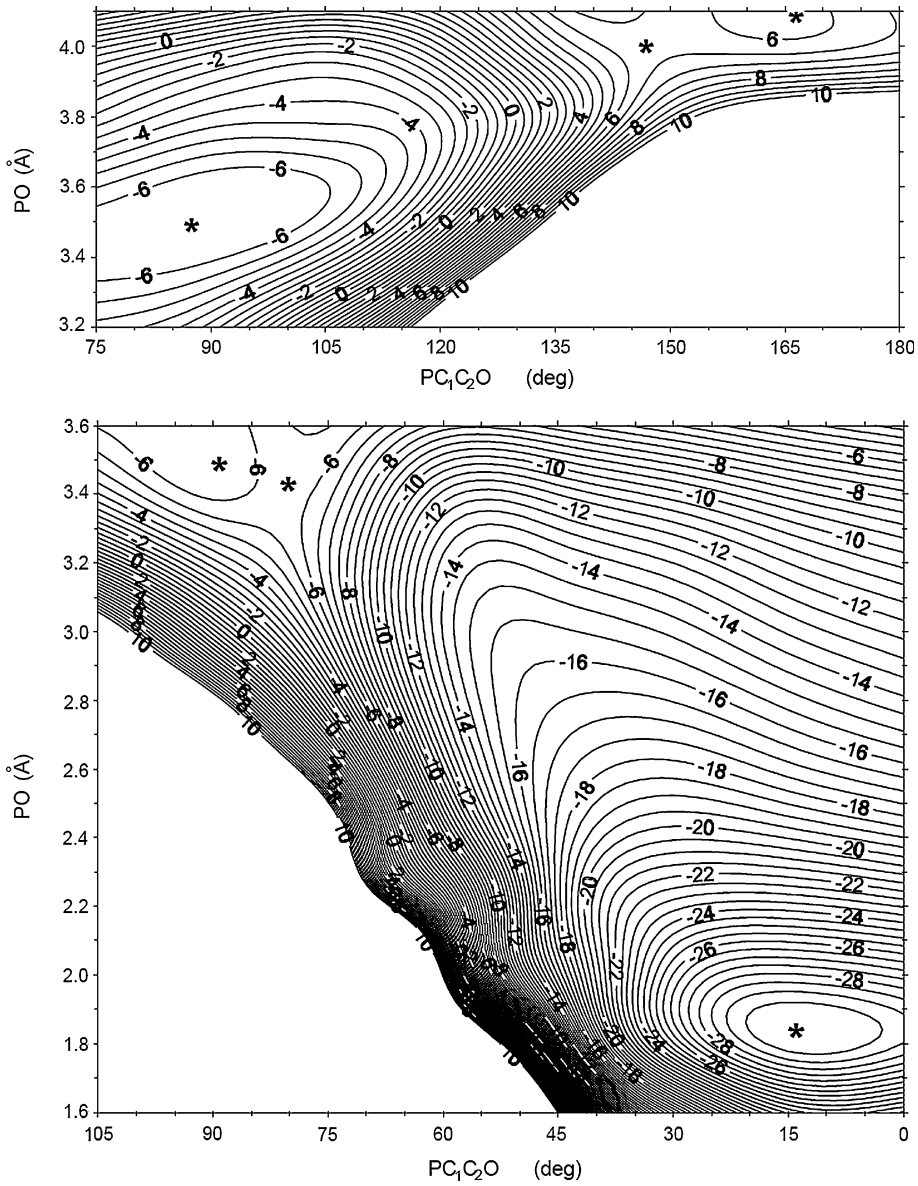

Fig. 12 B3P86/6-31G* potential energy surfaces in vacuo using PC_1C_2O and PO as leading parameters: anti to gauche betaine-type intermediate (Ba to Bg, *top*) and gauche betaine-type intermediate to oxaphosphetane (Bg to OP1, *bottom*). The *asterisks* stand for the stationary points. The TS imaginary frequencies are −11.88 and −19.38 cm^{-1} for Bg–Ba and Bg–OP1, respectively. Isopotential lines spaced by 0.5 kcal/mol (lines above 10 kcal/mol not drawn)

(that might be narrow) about OP1 and a transition state nearly as high as the reactant adduct.

Including zero point and thermal corrections in solution (referred to the isolated reactants, but consistently shifted when Reac was moved to zero), the most outstanding difference with respect to the rigid geometry free energy profile, displayed in Fig. 8, is the absence of TS1 and OP2, whereas the relative positions of Reac, OP1 and TS2 are similar. Reac(T) derived from the minimization of one of the reactant adducts obtained in THF starting from TS1.

3.3 Stepwise reaction mechanism in vacuo

The Wittig reaction had been described for years as a stepwise ionic process involving a betaine-type intermediate with oxaphosphetanes on the path to the final product. When solvent effects supported a nonpolar transition state in some cases [48], the debate about the mechanistic aspects of this reaction started, while oxaphosphetanes were soon after indicated as the only observable intermediates in a number of Wittig reactions [49].

For our diastereomeric aldehyde, the lowest energy (−6.59 kcal/mol) betaine-type intermediate, that can be reached from the Reac(B) reactant adduct via the TSb transition state, presents a gauche structure (Bg), displayed in Fig. 10 together with TSb (iF = −103.23 cm^{-1}).

Relative stabilities and a number of geometrical parameters are reported in Table 4. The relative energy profile along this path is shown in Fig. S1 of the Electronic Supplementary Information.

Once the Bg structure had been located, the flexible scan about PC_1C_2O was performed to evaluate the relative

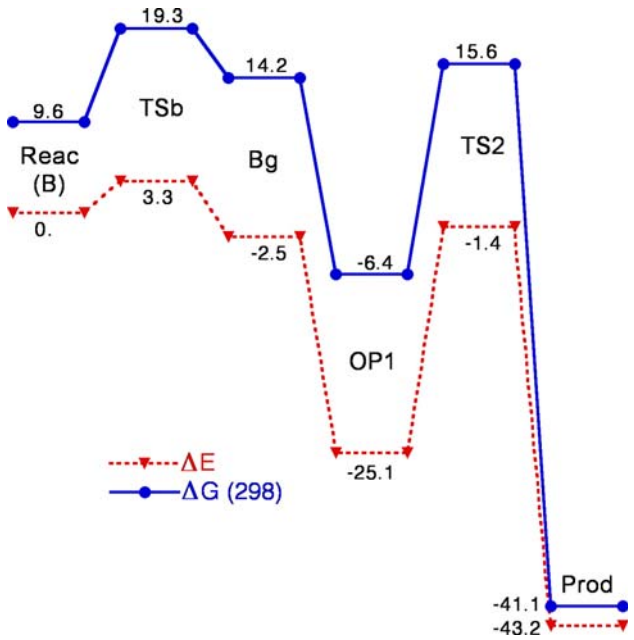

Fig. 13 B3P86/6-31G* profiles (kcal/mol) along the stepwise pathway in vacuo: potential energy, ΔE (*dotted line*, *down triangles*) and free energy, ΔG (*solid line*, *circles*)

stability of the various rotamers sketched in Fig. 2. From the plot of Fig. 11, it is evident that Bg is the lowest energy betaine-type intermediate.

The syn rotamer (Bs) actually does not exist, because for $-60° \leq PC_1C_2O \leq 60°$ the betaine-type structure moves to an oxaphosphetane-type arrangement spontaneously and at PC_1C_2O values in the region of 0° an OP four-center intermediate is invariably obtained during the optimizations. Conversely, the anti rotamer (Ba) is stable at this level, although much less favorable (by $\sim$12 kcal/mol) than Bg, despite previous studies reached opposite conclusions [50, 51], ruling out the presence of anti betaine in vacuo. The changes in $P\cdots O$ and $C_1\cdots C_2$ occurring during the rotation about PC_1C_2O are displayed in Fig. S2 of the ESI.

In order to clarify the behavior of the betaine-type structures in vacuo, the PES for the rotation about PC_1C_2O at various PO separations has been investigated both for the Ba–Bg (top) and Bg–OP1 (bottom) pathways. The stationary points are indicated with asterisks on the PES, displayed in Fig. 12.

The profile displayed in Fig. 11 corresponds to the minimum energy paths on both surfaces where actually the TS is very close to Ba (top) and Bg (bottom).

The potential energy (ΔE) profile including Bg, the betaine-type intermediate, displayed in Fig. 13, passes through OP1 (as clearly indicated by Figs. 11, 12 as well as by several other geometry minimizations all eventually leading to TBP structures with O in apical position) to yield the olefin. Therefore, only the initial mechanism, being just slightly less favorable than the fully concerted one (Fig. 7), differs from it.[7] Bg has almost the same energy as TS2. As far as the free energy is concerned, Reac(B) is $\sim$1.2 kcal/mol more stable than the concerted mechanism Reac adduct, while the TSb barrier is $\sim$0.8 kcal/mol higher than that of TS1. Bg is more stable than TS2 in vacuo by $\sim$1.1 kcal/mol.

3.4 Stepwise reaction mechanism in THF

The rigid geometry profiles in solution have not been displayed because of the remarkable difference found above with respect to the relaxed ones.

Optimizing in THF solution we have not been able to locate neither TSb (probably its barrier is too low to be determined, as argued above for TS1 and OP2) nor a syn betaine (Bs). Conversely, two betaine-type intermediates, Bg and Ba, reported in Table 5, have been found to be stable in THF, with Ba more than 8 kcal/mol higher in energy than Bg. Therefore, Ba experienced a beneficial solvent effect amounting to about 4 kcal/mol. However, only Bg has been included in the plot. Noteworthy, a very low barrier should separate Bg from OP1 in THF.

The overall trend of the stepwise mechanism profile in THF, displayed in Fig. 14 (superimposed to the potential energy one in vacuo), does not significantly differ from the concerted mechanism ΔG_{tot} profile in THF of Fig. 9, apart the presence of Bg along the downhill path to OP1. This trend is probably due to the low dielectric constant of THF.

Increasing the polar character of the solvent indeed, a decidedly larger propensity toward betaine-type intermediates was found with model systems, i.e. Me_3PCH_2 and MeCHO, in dimethylsulfoxide (DMSO, $\varepsilon = 46.7$), where on the contrary oxaphosphetane is destabilized [23].

From the profiles of both mechanisms in THF, a clear preference for either pathway cannot be put forward, although the stepwise mechanism cannot be ruled out. Based on quantum molecular dynamics simulations in DMSO of model systems, Ziegler and co-workers [23] assume that the path leading to OP1 is alternative to the betaine-type one, thus excluding OP1 from the pathway. Conversely, from our results on a bulky chiral aldehyde and Ph_3PCH_2 in vacuo and in THF, we cannot discard OP1, because it was encountered at the end of most minimizations while every effort to get a syn betaine invariably lead to it.

[7] OP2 was not reported on this plot to avoid its artifactual presence in the subsequent plots in THF solution where it is unstable.

Table 5 IEF-PCM/B3P86/6-31G* relative total free energies in THF and geometrical parameters of betaine-type structures

System	ΔG_{tot}	PC_1	PO	C_1C_2	C_2O	PC_1C_2O	POC_2C_1	$\Delta G_{tot}(298)$
Reac(B)	2.009	1.701	4.854	3.206	1.215	79.90	−16.91	12.31
Bg	−6.422	1.819	3.553	1.591	1.336	90.69	−34.80	10.20
Ba	1.920	1.830	4.092	1.614	1.325	166.66	−8.05	19.47
OP1	−22.252	1.866	1.845	1.527	1.414	10.73	−10.90	−4.20

Relative free energies (kcal/mol), distances (Å), angles (deg); reference values in Table 3

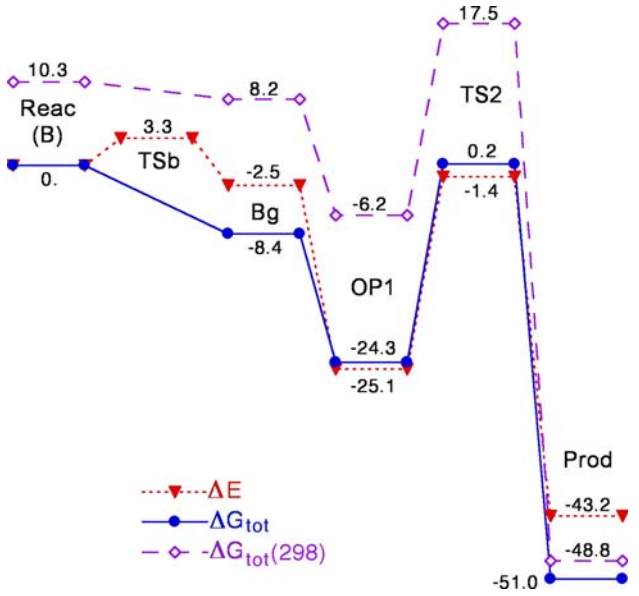

Fig. 14 IEF-PCM/B3P86/6-31G* free energy profiles along the stepwise path in THF: ΔG_{tot} (*solid line*, *circles*) and $\Delta G_{tot}(298)$ after including ZPE and thermal corrections (*dashed line*, *diamonds*); the potential energy in vacuo, ΔE (*dotted line*, *down triangles*), is also displayed (kcal/mol)

4 Conclusions

The Wittig reaction has been investigated with computational methods at the B3P86/6-31G* level in vacuo and in THF solution in the polarizable continuum model framework (IEF-PCM). Although no constraints have been imposed, the presence of bulky groups at P and on the aldehyde produced puckered TS, with PCCO $\approx$ 40°.

The concerted path via oxaphosphetane intermediates features a transition state (TS1) between the reactant adduct and OP1, a TBP structure with O and one of the phenyl rings in apical positions. Pseudorotation of the substituents at P gives OP2, on the uphill pathway to TS2. OP2 as such cannot be found under different conditions (i.e. in THF solution) and it is very close to a TS structure. A remarkable TS (TS2) is located between OP1 and the final products (olefin + triphenylphosphoxide). As observed also in other cases, the free energy heavily depends on the system molecularity, being very close to the potential energy when two separate molecules are considered, whereas there is a significant increase in the free energy when adducts or complexes are considered.

Using the in vacuo geometries, the energy profile in THF solution is maintained with limited changes among the various species. Conversely, geometry optimizations in solution lead to a very different profile, because a number of species (such as TS1, OP2 or Ba) are not locatable in THF, probably because the barrier separating them from nearby stable structures is too low.

The stepwise profile (i.e. the path involving a betaine-type intermediate) is nearly as favorable as the concerted one in solution.

Acknowledgments This article is dedicated to Prof. Oriano Salvetti, who pervaded most of our lives with his presence: he was one of our University teachers and for a number of years the director of ICQEM-CNR, our former Institute.

References

1. Wittig G, Geissler G (1953) Liebigs Ann Chem 580:44–57
2. Wittig G, Schöllkopf U (1954) Chem Ber 87:1318–1330
3. Wittig G, Haag W (1955) Chem Ber 88:1654–1666
4. Vedejs E, Snoble KAJ, Fuchs PL (1973) J Org Chem 38:1178–1183
5. Vedejs E, Meier GP, Snoble KAJ (1981) J Am Chem Soc 103:2823–2831 (and references quoted therein)
6. Vedejs E, Marth CF, Ruggeri R (1988) J Am Chem Soc 110:3940–3948
7. Vedejs E, Marth CF (1988) J Am Chem Soc 110:3948–3958
8. Vedejs E, Marth CF (1990) J Am Chem Soc 112:3905–3909
9. Schlosser M, Schaub B (1982) J Am Chem Soc 104:5821–5823
10. Schröder U, Berger S (2000) Eur J Inorg Chem 2601–2604
11. Appel M, Blaurock S, Berger S (2002) Eur J Inorg Chem 1143–1148
12. Kojima S, Sugino M, Matsukawa S, Nakamoto M, Akiba K (2002) J Am Chem Soc 124:7674–7675
13. Restrepo-Cossio AA, Cano H, Marí F, Gonzalez CA (1997) Heteroatom Chem 8:557–569
14. Restrepo-Cossio AA, Gonzalez CA, Mari F (1998) J Phys Chem A 102:6993–7000 (and references quoted therein)
15. Naito T, Nagase S, Yamataka H (1994) J Am Chem Soc 116:10080–10090
16. Yamataka H, Nagase S (1998) J Am Chem Soc 120:7530–7536
17. Robiette R, Richardson J, Aggarwal VK, Harvey JN (2005) J Am Chem Soc 127:13468–13469

18. Robiette R, Richardson J, Aggarwal VK, Harvey JN (2006) J Am Chem Soc 128:2394–2409
19. Peralta Pérez E, López Ortiz F (2000) Chem Commun 2029–2030
20. Höller R, Lischka H (1980) J Am Chem Soc 102:4632–4635
21. Lu WC, Wong NB, Zhang RQ (2002) Theor Chem Acc 107:206–210
22. Kalaiselvan A, Venuvanalingam P (2005) Tetrahedron Lett 46:4087–4090
23. Seth M, Senn HM, Ziegler T (2005) J Phys Chem A 109:5136–5143
24. Maercker A (1965) Org React 14:270–490
25. Maryanoff BE, Reitz AB (1989) Chem Rev 89:863–927
26. Johnson AW (1993) Ylides and imines of phosphorus. Wiley, New York
27. Walker BJ (1996) Organophosphorus Chem 27:264–307
28. Alagona G, Ghio C (in preparation) Dependence of the Wittig reaction mechanism on the environment and on the substituents at the aldehyde group and at the phosphonium ylide
29. Settambolo R, Rocchiccioli S, Uccello-Barretta G, Lazzaroni R (2007) Lett Org Chem 4:388–392
30. Frisch MJ, Trucks GW, Schlegel HB, Scuseria GE, Robb MA, Cheeseman JR, Montgomery JA Jr, Vreven T, Kudin KN, Burant JC, Millam JM, Iyengar SS, Tomasi J, Barone V, Mennucci B, Cossi M, Scalmani G, Rega N, Petersson GA, Nakatsuji H, Hada M, Ehara M, Toyota K, Fukuda R, Hasegawa J, Ishida M, Nakajima T, Honda Y, Kitao O, Nakai H, Klene M, Li X, Knox JE, Hratchian HP, Cross JB, Bakken V, Adamo C, Jaramillo J, Gomperts R, Stratmann RE, Yazyev O, Austin AJ, Cammi R, Pomelli C, Ochterski JW, Ayala PY, Morokuma K, Voth GA, Salvador P, Dannenberg JJ, Zakrzewski VG, Dapprich S, Daniels AD, Strain MC, Farkas O, Malick DK, Rabuck AD, Raghavachari K, Foresman JB, Ortiz JV, Cui Q, Baboul AG, Clifford S, Cioslowski J, Stefanov BB, Liu G, Liashenko A, Piskorz P, Komaromi I, Martin RL, Fox DJ, Keith T, Al-Laham MA, Peng CY, Nanayakkara A, Challacombe M, Gill PMW, Johnson B, Chen W, Wong MW, Gonzalez C, Pople JA (2004) Gaussian 03, Revision C.02. Gaussian Inc., Wallingford
31. Becke AD (1993) J Chem Phys 98:5648–5652
32. Perdew JP (1986) Phys Rev B 33:8822–8824
33. Hehre WJ, Radom L, Schleyer PVR, Pople JA (1986) Ab initio molecular orbital theory. Wiley, New York
34. Alagona G, Ghio C, Lazzaroni R, Settambolo R (2001) Organometallics 20:5394–5404
35. Alagona G, Ghio C (2005) J Organomet Chem 690:2339–2350
36. Alagona G, Ghio C, Rocchiccioli S (2007) J Mol Model 13:823–837
37. Lazzaroni R, Settambolo R, Marchetti M, Paganelli S, Alagona G, Ghio C (2008) Inorg Chim Acta. doi:10.1016/j.ica.2008.07.006
38. Alagona G, Ghio C (in preparation)
39. McQuarrie DA (2000) Statistical mechanics. University Science Book, Sausalito
40. Tomasi J, Persico M (1994) Chem Rev 94:2027–2094
41. Barone V, Cossi M, Tomasi J (1997) J Chem Phys 107:3210–3221
42. Cancès E, Mennucci B, Tomasi J (1997) J Chem Phys 107:3032–3041
43. Cancès E, Mennucci B (1998) J Chem Phys 109:249–259
44. Cancès E, Mennucci B, Tomasi J (1998) J Chem Phys 109:260–266
45. Amovilli C, Barone V, Cammi R, Cancès E, Cossi M, Mennucci B, Pomelli CS, Tomasi J (1998) Adv Quantum Chem 32:227–261
46. Tomasi J, Mennucci B, Cammi R (2005) Chem Rev 105:2999–3094
47. Bondi A (1964) J Phys Chem 68:441–451
48. Frøyen P (1972) Acta Chem Scand 26:2163–2168
49. Vedejs E, Snoble KAJ (1973) J Am Chem Soc 95:5778–5780
50. Volatron F, Eisentein O (1987) J Am Chem Soc 109:1–14
51. Piskala A, Rehan AH, Schlosser M (1983) Collect Czech Chem Commun 48:3539–3551